Cooling Rate Effect on Microhardness for SAW Welded Mild Steel Plate

Harish Arya, Kulwant Singh & Sanjay Singh

Department of Mechanical Engineering, Sant Longowal Institute of Engineering and Technology
Longowal, Sangrur -148106 India
E-mail : arya.iitr@gmail.com, erkulwant@yahoo.co.in, slietsanjaysingh@gmail.com

***Abstract* – During fusion welding process it is possible to determine temperature at any point by using thermocouples and from such data it is possible to draw temperature distribution for any point of interest, such temperature distribution can be utilized to determine average cooling rate and distortion. These studies are utilized to investigate the microstructure and microhardness of the heat affected zone (HAZ) and weldment. In present work, the influence of heat input and temperature distribution on microstructure and mechanical properties of weldment have been investigated. Fractional factorial design technique is used to conduct the experiment with four factors and two levels. Eight combinations and two set of heat input are designed with different combinations of SAW welding parameters. Temperature distribution curves and cooling rate, distortion, and microhardness curve have been drawn. The effects of selected welding parameters on the microhardness and microstructure have been investigated.**

Keywords – microhardness, microstructure, Submerged arc Welding, Temperature distribution, cooling rate

I. INTRODUCTION

Boiler and pressure vessel plate SA- 516 grade 70 have been widely used in Boilers and pressure vessels, boats, bridges, wind turbine towers, oil and gas pipelines. Boiler and pressure vessel plate are the most important structural materials for construction because of their high strength and toughness and relatively low cost. Welding is the most reliable, efficient and practical metal joining process which is widely used in industries such as nuclear, aerospace, automobile, transportation, and off-shore. In spite of the many advantages, there are some limitations affecting this process. Welding defects influence the desired properties of welded joints. Temperature distribution significantly affects parameters such as residual stresses, distortions, weld microstructure, HAZ hardness. Because of local heating during welding process, controlling the temperature distribution is critical. That will be present in the material after cooling to room temperature. Very limited experimental data regarding temperature distribution during multipass welding plate is available in literature.

II. EXPERIMENTATION

The material of plate selected for the present work is SA-516 grade 70 i.e. boiler and pressure vessel plate. Typical chemical composition of the plates used in the experiments work is given in the table 1. Two plate of size 300*75*12 are used with a single V- groove joint prepared with the help of shaper machine. The plates are tacked by TIG welding before commencing welding with a uniform gap of 2.4 mm between the plates as per ASME SECTION IX-guide QW 402.1.10. The welding process selected for present experimental work was submerged arc welding (SAW). Thermocouples (K-type) were used to measure the transient temperature distribution during welding. The thermocouples were fixed in the equal distance from the weld center line. The dimensional details of plates and position of thermocouples are shown in Fig. 1. The temperature distributions during experimentation were recorded by temperature meter. 'KERC' Submerged Arc Welding equipment, type ASA-I, has been used with a power source WR-1200-H for multipass welds. The electrode wire used for the welding was Auto melt Grade - A of 3.15 mm diameter conforming to AWS SFA 5.17, EL-08. An agglomerate flux is used in this investigation. The specification of flux used for welding is AWS 5.17 OK FLUX 10.71 L, F7AZ - EL 8. The interpass temperature was considered for experimental work is the 150^0C as per ASME-IX 5.17. During multipass welding, temperature is measured as a function of time. These readings of temperature are useful to draw temperature distribution. The temperature was measured until the weld reach to the room temperature.

TABLE I- CHEMICAL COMPOSITION OF PLATE

Element	C	Mn	S	P	Si	ferrous
%	0.20	0.75	0.035	0.035	0.016	Rest.

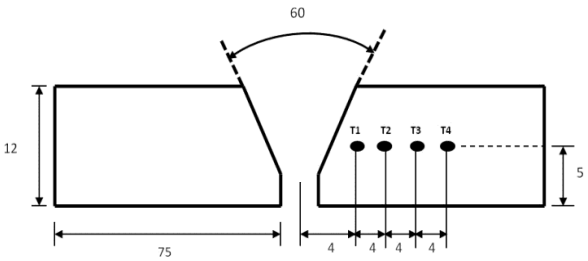

Fig. 1 : Plate dimension and thermocouple position

III. METHODOLOGY

The Experiments carried out in the following steps

A. Preparation of base plate

B. Identifying the important process parameters and their limits.

C. Developing the design matrix.

D. Conducting the experiments as per the design matrix.

E. Measurement of temperature during experimentation.

F. Calculating the cooling rate, distortions, microhardness of weld bead and HAZ

The selected process parameters were arc voltage (V), welding current(I), welding speed (S), and nozzle to plate distance(NTPD). Trial runs carried out according to the design matrix as shown in table 3. The working range was decided upon by inspecting the bead for smooth appearance without any visible defects and heat input tolerate by root pass. The upper limit of a factor was coded as +1 and the lower limit as - 1. The process variables with their units and notations are given in table 2.

TABLE 2 - WELDING PROCESS PARAMETERS

Parameters	Units	Notations	Lower limits	Higher limits
Welding current	Amp	I	300	350
Arc voltage	Volts	V	30	38
Welding speed	Mm/min	S	256	550
Nozzle to plate distance	mm	NTPD	18	22

TABLE 3: DESIGN MATRIX

Trial No.	I	V	S	N
	1	2	3	4=123
1.	+1	+1	+1	+1
2.	-1	+1	+1	-1
3.	+1	-1	+1	-1
4.	-1	-1	+1	+1
5.	+1	+1	-1	-1
6.	-1	+1	-1	+1
7.	+1	-1	-1	+1
8.	-1	-1	-1	-1

IV. TEMPERATURE DISTRIBUTION

Figure 1 to Figure 8 shows the temperature distribution of welded joints, welded at different combination of process parameters. Table 4 shows the different combinations of process

Temperature distribution at high heat input with single pass

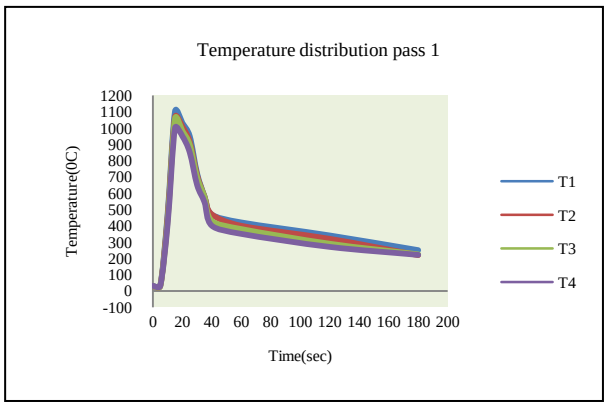

Temperature distribution at medium heat input with two pass

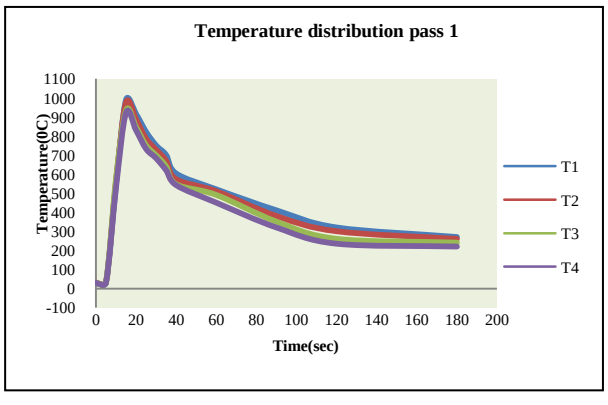

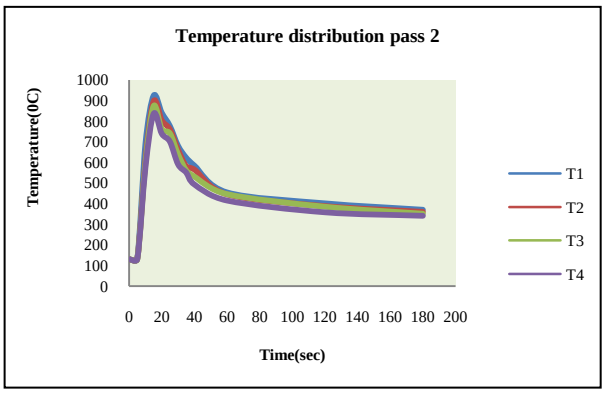

Temperature distribution at low heat input with six passes

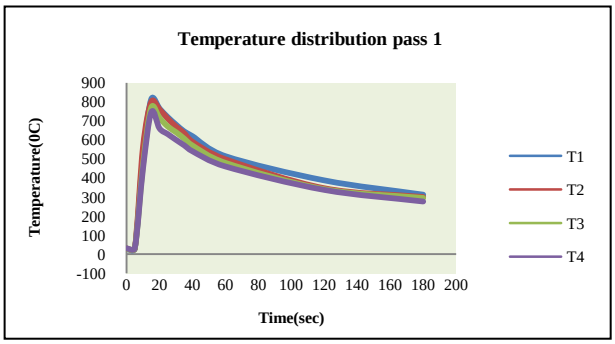

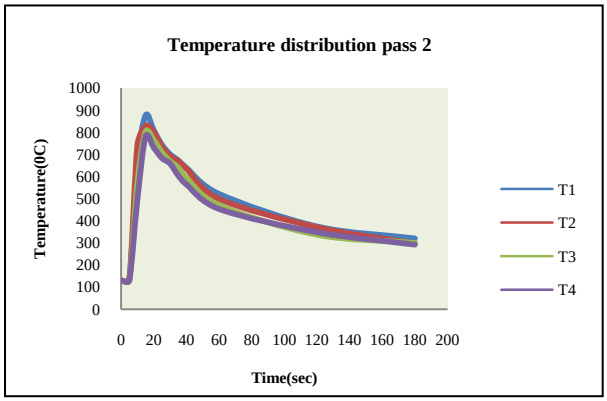

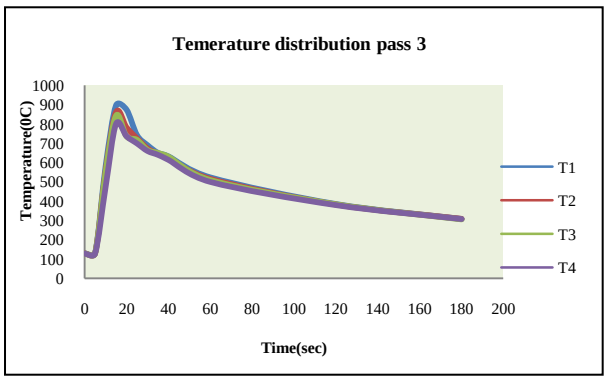

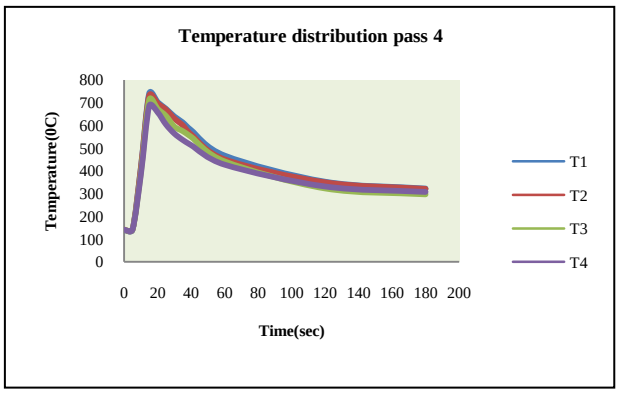

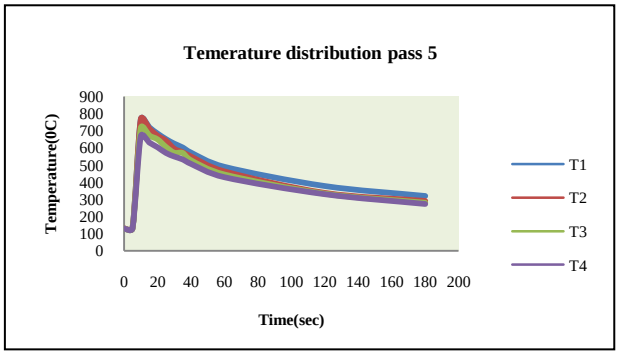

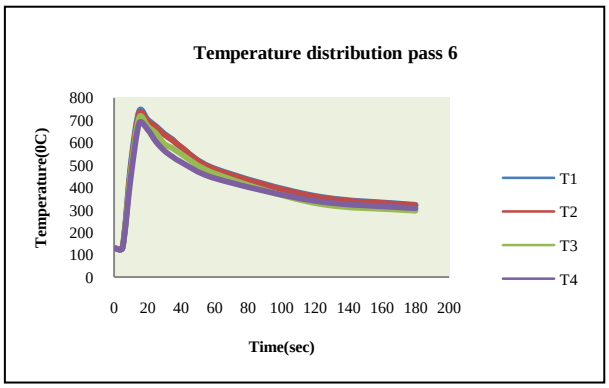

IV. COOLING RATE

The average cooling rate is calculated in multipass welding from 800^0C to 500^0C, because this temperature range is useful to phase transformation. It is observed that when the number of passes increased, the total heat input is increased vice-versa; the average cooling rate of weldment is reduced. The average Cooling rate is calculated by the equation 1 and Table 4 shows the calculated total heat input and average cooling rate. Heat input per pass is calculated from welding parameters and average cooling rate is calculated from temperature distribution in every pass in welding.

$$\text{Cooling rate} = \frac{\text{Temp range from } 800^0\text{C to } 500^0\text{C}}{\text{Time taken from } 800^0\text{C to } 500^0\text{C during cooling}}$$

The result shows that Cooling rate plays a key role on the phase balance in the HAZ and weld. It also significantly affects the formation of inter-metallic phases. The larger number of weld beads in a similar cross sectional area resulting in additional temperature distribution at the higher cooling rate contributed to Microstructural refinement and a more uniform hardness in the weld metal.

TABLE 4 - HEAT INPUT AND COOLING RATE

Heat input in KJ/mm	No. of passes	Total heat input in KJ/mm	Av. Cooling rate in ^{0}C/sec
0.981	6	5.886	2.75
2.669	2	5.338	4.5
3.381	1	3.381	6.15

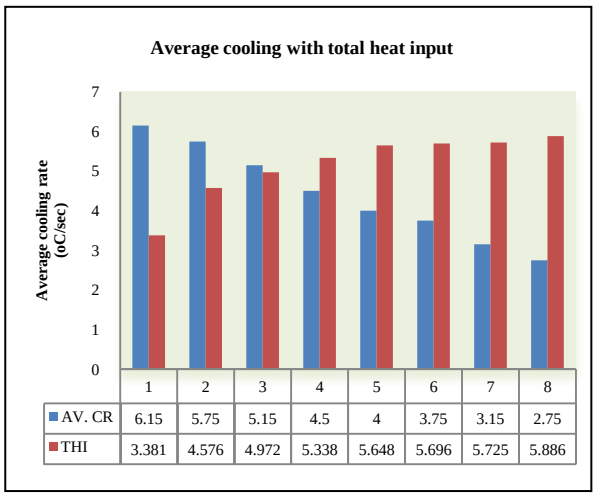

V. MICROHARDNESS

Three specimen were selected according to the total heat input (low, medium and high cooling rate) for further study of microhardness. Figure shows the microhardness curve of three specimens with different heat input. There were 11 points where the microhardness was tested and '0' point at horizontal axis in the shows the centre points of the weld bead and '11th' point is at horizontal axis shows that the microhardness is taken at base metal from right side of the weld bead. Peak of each curve in Figure 11 shows the fusion boundary of weld bead. Right and left end of each curve indicate the base metal as well as HAZ respectively. Microhardness of weldment at low heat input is higher at all points (weld metal and HAZ) as compare to the weldment at Medium and high heat input.

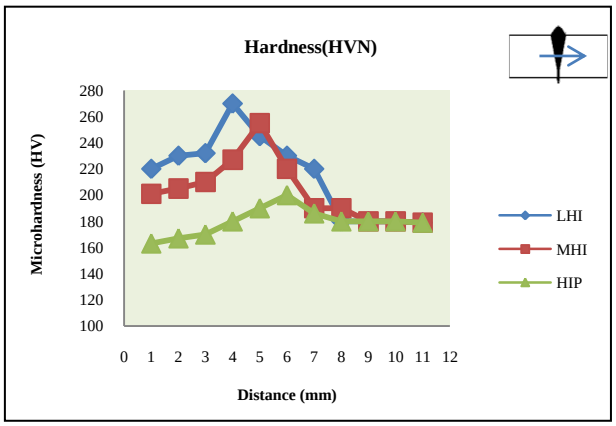

Fig. 11

VI. ANGULAR DISTORTION

During the heating cycle, localized heating induces non-uniform expansion, which is concentrated in the part in and near the welding pass and is constrained by the surrounding parts. During the cooling cycle, shrinkage of the heated part occurs when heating has stopped. Plastic deformation takes place due to the unevenness of the temperature fields, the restraining effects of the structure, and variations in the material properties that occur during the heating and cooling cycle. Plastic deformation remains after welding is completed. There specimens are selected according to the total heat input for further study of distortion. Figure 12 shows the distortion verses total heat input curve.

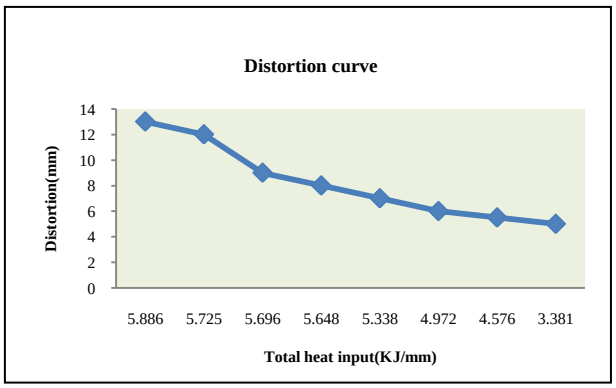

Fig. 12

VII. MICROSTRUCTURE

The effect of multipass welding on the microstructure of the weld metal was that grain size increased at the reheated portion of the weld metal. In

the multilayer welds, the thermal effect of upper runs had a tendency to normalize the structure of those previously solidified, leading to a refinement of the structure and thus giving variation in the hardness values in these zones**.** The presence of a repetitive microstructure consisting of columnar grain, coarse and fine grained ferrite and pearlite, unaffected structure within the weld zone confirms that there is a significant modification of microstructure due to multiple passes.

Figure of micrograph of the weldment with different heat input (high, medium, low). At the number of passes increase, the total heat input increase, the grains HAZ are larger in size due to repeated heating and grain refinement as compared to the weldment having Medium and low heat input in multipass welding. By the faster cooling rate finer grains are formed and fine grains produce the higher hardness.

TABLE 5 - MICROHARDNESS OF WELD METAL AND HEAT AFFECTED ZONE

HI/pass	Total HI	Av. CR.	Av. Microhardness of WM	Av. Microhardness of HAZ
0.981	5.886	2.75	229.5	238.5
2.669	5.338	4.5	193.5	216
3.381	3.381	6.15	159.5	176

Columnar grains are formed in weldment. The larger columnar grains are formed by high heat input as compared to medium and low heat input. It is also observed that the coarse grains is more in the weldment with high heat input, results the less hardness. Microstructure shows columnar grains at weld bead and coarse grain of pearlite at HAZ in high heat input and medium heat input. Microstructure shows columnar grains at weld bead and coarse grains of pearlite and ferrite at HAZ in low heat input. It can be observed that columnar grains coarsen with the increase of heat input. Each weld pass shows different orientation of the grains. Grains are mostly coarse and cellular near centreline of the bead. In multipass welding fusion zones of a weld of weld pass is replaced by HAZ of subsequent passes which is evident from the micrographs. Primarily shows two phases namely ferrite (light etched) and pearlite (dark etched) and fine carbide particles are not visible at low magnification. Grain coarsening near the fusion boundary (in HAZ) results in coarse columnar grains in the weld metal. An increase in heat input increased the average size of different phase present in the weld metal and weld centre line shows columnar dendrites structure.

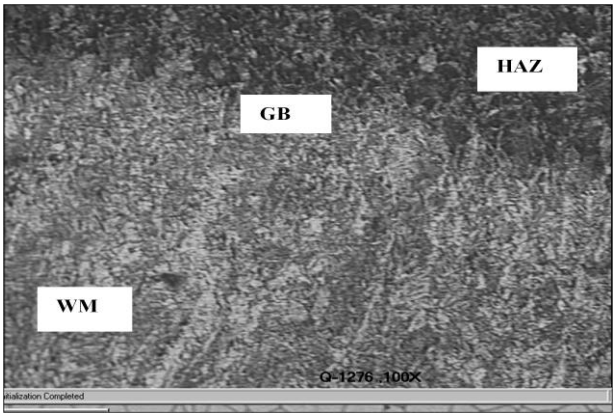

(a) Low Heat Input

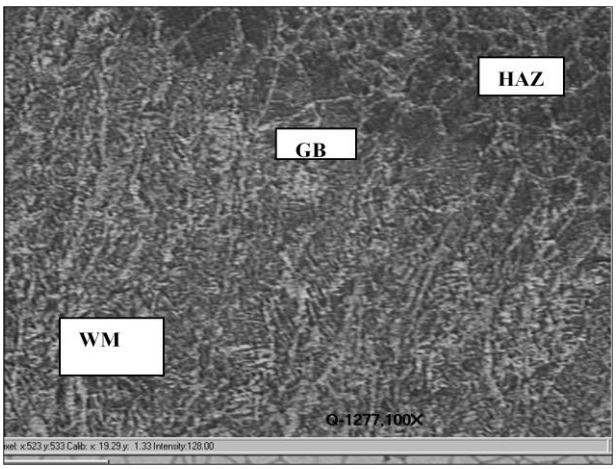

(b) Medium Heat Input

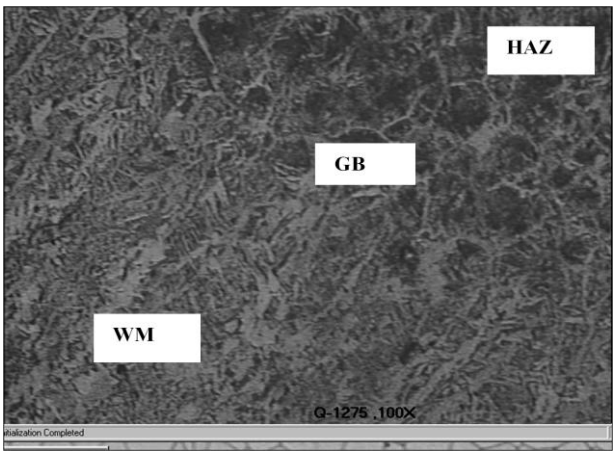

(c) High Heat Input

VIII. RESULT AND DISCUSSION

1. As expected, during each pass of the weld the temperature at the measuring point increases, reaches a maximum value and the decreases. The

point that is nearest to the weld pad centre line reaches the highest maximum temperature.

2. It can be seen that heat input increases as well as temperature increases. Temperature attained in each pass is different due the effect of interpass temperature and heat input.

3. It is observed from figure that with the increasing in number of pass as well as total heat input from 3.381 KJ/mm to 5.886 KJ/mm the average cooling rate is reduced from 6.15^0C/sec to 2.75^0C/sec.

4. Microhardness of weldment at low heat input is higher at all points (weld bead and HAZ) as compare to the weldment at Medium and high heat input. When the heat input was low (3,381 KJ/mm) the maximum hardness value (270 VHN) at fusion boundary was observed as compared to the hardness (186 VHN) achieved by high heat input (5.886 KJ/mm).

5. It is observed that the hardness is higher in the HAZ than the weld metal. With increasing cooling rate, hardness increases by 4.29% in the weld metal and 3.33% in the HAZ at cooling rate 2.750°C/sec and hardness increases by 2.20% in weld metal and 2.97% in the HAZ at cooling rate 6.150°C/sec.

6. It is observed from the multipass welding that the number of passes increases, the total input increases from 3.381KJ/mm to 5.886 KJ/mm as well as the distortion increased 5 mm to 13mm.The distortion is higher at high heat input and the total distortion increases by 61.53% and 7.69 times.

7. In multipass welding fusion zones of a weld pass is replaced by HAZ of subsequent passes which is evident from the micrographs. Primarily shows two phases namely ferrite (light etched) and pearlite (dark etched) and fine carbide particles are not visible at low magnification. Grain coarsening near the fusion boundary (in HAZ) results in coarse columnar grains in the weld metal. An increase in heat input increased the average size of different phase present in the weld metal and weld centre line shows columnar size structure. It is observed from multipass submerged arc welding more ferritic structures are observed for low heat input with more number of welding passes and rapid cooling rate whereas more graphite structure are observed at high heat input due less number of passes and slow cooling rate. Percentage of ferrite increases due to more refined grains as the number of passes is more at low heat input. Whereas for increasing heat input percentage of graphite and pearlite is decreased and ferrite increased which result better mechanical properties. The increases in ferrite phase due to change of temperature distribution the hardness of HAZ increase and weld metal hardness decreases.

8. It is also observed by macrostructure at "10X" that the weld bead width formed by the high total heat input (5.886 KJ/mm) is bigger than the weld bead width formed by the low total heat input (3.381 KJ/mm) and width of HAZ is also increased by increasing, the number of passes and heat input in multipass welding.

Knowledge of maximum temperature rise will be useful in the estimation of maximum temperature attained by different region of the base plate during multipass welding. Likely change in the microstructure and consequently degradation in mechanical property can be estimated from the information.

IX. REFERENCES

[1] S. M. Metev and V. P. Veiko, Laser Assisted Microtechnology, 2nd ed., R. M. Osgood, Jr., Ed. Berlin, Germany: Springer-Verlag, 1998.

[2] J. Breckling, Ed., The Analysis of Directional Time Series: Applications to Wind Speed and Direction, ser. Lecture Notes in Statistics. Berlin, Germany: Springer, 1989, vol. 61.

[3] S. Zhang, C. Zhu, J. K. O. Sin, and P. K. T. Mok, "A novel ultrathin elevated channel low-temperature poly-Si TFT," IEEE Electron Device Lett., vol. 20, pp. 569–571, Nov. 1999.

[4] M. Wegmuller, J. P. von der Weid, P. Oberson, and N. Gisin, "High resolution fiber distributed measurements with coherent OFDR," in Proc. ECOC'00, 2000, paper 11.3.4, p. 109.

[5] R. E. Sorace, V. S. Reinhardt, and S. A. Vaughn, "High-speed digital-to-RF converter," U.S. Patent 5 668 842, Sept. 16, 1997.

[6] (2002) The IEEE website. [Online]. Available: http://www.ieee.org/

[7] M. Shell. (2002) IEEEtran homepage on CTAN. [Online]. Available: http://www.ctan.org/tex-archive/macros/latex/contrib/supported/IEEEtran/

[8] FLEXChip Signal Processor (MC68175/D), Motorola, 1996.

[9] "PDCA12-70 data sheet," Opto Speed SA, Mezzovico, Switzerland.

[10] A. Karnik, "Performance of TCP congestion control with rate feedback: TCP/ABR and rate adaptive TCP/IP," M. Eng. thesis, Indian Institute of Science, Bangalore, India, Jan. 1999.

[11] J. Padhye, V. Firoiu, and D. Towsley, "A stochastic model of TCP Reno congestion avoidance and control," Univ. of Massachusetts, Amherst, MA, CMPSCI Tech. Rep. 99-02, 1999.

[12] Wireless LAN Medium Access Control (MAC) and Physical Layer (PHY) Specification, IEEE Std. 802.11, 1997.

◈◈◈

.